JOURNAL OF GEOPHYSICAL RESEARCH, VOL. 102, NO. A8, PAGES 17,233-17,240, AUGUST 1, 1997

Modulated Langmuir waves: Observations from Freja and SCIFER

J. Bonnell and P. Kintner

School of Electrical Engineering, Cornell University, Ithaca, New York

J.-E. Wahlund

Swedish Institute of Space Physics, Kiruna Division, Kiruna

J. A. Holtet

Department of Physics, University of Oslo, Oslo

Abstract. Modulated Langmuir waves were commonly observed using the HF waveform-capture instruments on the Freja satellite and SCIFER sounding rocket in the terrestrial auroral zone. The modulation frequency of the Langmuir waves during several hundred events was estimated, and found to extend routinely to several tens of kilohertz. Using the linear dispersion relation for oblique Langmuir waves in the $f_{pe} < f_{ce}$ domain, these modulation bandwidths were found to correspond to interactions between waves at significantly larger angles to each other, and to $\mathbf{B_0}$, than typically treated in theoretical analyses of Langmuir wave modulations. A model of the modulation based on scattering via electrostatic whistler/lower hybrid waves is proposed as a viable explanation of the broad modulation bandwidth.

Introduction

Large amplitude, narrow-band emissions at the local plasma frequency have been reported frequently in sounding rocket probes of the auroral zone. Initial work which investigated the coherent amplification of electrostatic whister band noise by the precipitating keV auroral electron beam [*Maggs*, 1978] predicted that large amplitude emissions would be seen at the local plasma frequency when $f_{pe} < f_{ce}$. Some such emission at tens of mV/m was observed in the bulk of keV inverted-V precipitation [*McFadden et al.*, 1986]. The strongest emission events (hundreds of mV/m) were not observed in the body of the inverted-V arcs, but were instead observed on the edges of the arcs during periods when the electron precipitation was of the form of a narrow field-aligned beam at energies of a few 100 eV. The envelope of these narrow-band emissions was measured, and was found to be modulated at a few kilohertz. These observations suggested that some form of nonlinear process was producing the modulations, as it was unlikely that simple linear growth could produce waves with similar enough amplitudes and frequencies to explain the observed modulations. Several possible wave-wave and wave-particle nonlinearities have been suggested as playing a role in producing these modulations, ranging from parametric decay and modulational instabilities where the Langmuir waves decay to, or scatter off of ion acoustic or magnetized low-frequency ion modes (ion Bernstein or lower hybrid) [*Ergun et al.*, 1991; *Newman et al.*, 1994b], to kinetic wave-particle interaction models where particles trapped in the wave potential supply the low-frequency mode [*Muschietti et al.*, 1995; *Akimoto et al.*, 1996].

The observations of modulated Langmuir waves on Freja and SCIFER serve to expand the range of observations by exploring a broader range of the f_{pe}/f_{ce} parameter than has been reported in the literature; the reported observations deal with the regime $f_{pe} \approx f_{ce}$, the Freja and SCIFER observations cover the range $0 < f_{pe}/f_{ce} < 1$. We have taken a complementary approach to that of event studies such as *Stasiewitz et al.* [1996] in that we have examined the obvious modulational properties of a large number of events in order to look for scalings and distributions of those properties for comparison with theory.

In this paper, we will first describe the instrumentation used on Freja and SCIFER to observe the modulated Langmuir waves, and the relevant properties of that instrumentation to our study. We then describe how we determined the modulation frequency and other properties of each wave event. We will then present the results of our modulation study and show why those results argue for a model of modulated Langmuir waves involving the electrostatic whistler/lower hybrid mode. Finally, we will work out the resonance conditions for such a model and show that the predicted properties of

Paper number 97JA01499.
0148-0227/97/97JA-01499$09.00

Table 1. HF Instrument Properties

Property	Freja F4 HF	SCIFER HF
Probe size	2.5 cm diameter sphere	4.5 cm by 2.9 cm diameter cylinder
Probe separation	1.2 m	0.3 m
Capacitive attenuation	$\approx 1/4$	$\approx 1/5$
Sample rate	8 Msample/s	6.4 Msample/s
Resolution	8 bit	10 bit
Bandwidth	20 kHz to 4 MHz	2 kHz to 3.2 MHz

the electrostatic whistler/lower hybrid waves fit within a cold electrostatic model of those waves.

Instrumentation

The instruments used to observe Langmuir waves on Freja and SCIFER are quite similar in design. Each is a waveform capture device, which takes the continuously sampled signal from an electrostatic double-probe antenna, divides it into fixed-length snapshots, and transmits to ground a small fraction of the acquired snapshots on the basis of the broadband power of the signal within a snapshot. The relevant physical properties of the antennae, and the signal processing electronics of the two instruments are collected in Table 1. Further information on the Freja HF experiment may be found in the work of *Kintner et al.* [1995].

The coupling between the antenna probes and the ambient plasma is primarily capacitive at frequencies around f_{pe}, and the circuit consisting of the probe sheath and pre-amp input impedances creates a capacitive voltage divider which attenuates the measured electric field fluctuations from their values in the ambient plasma. For the double-probe antenna flown on Freja and SCIFER, this attenuation amounted to a factor of 2.5-4, based on the free space capacity of the probes, and the known capacity of the pre-amp circuits. The capacitance of the probe sheath will be decreased from the free space value by any space charge effects, which will increase the impedance of the sheath, and increase the attenuation. Therefore these values estimate the lower limit on the amplitude of the electric field fluctuations. This attenuation factor has been compensated for in the time series and power spectra presented later in this paper.

As has been shown by *Boehm et al.* [1994], the impedance of the probe sheath is a function of the potential across the sheath, making the sheath a nonlinear circuit element in which frequency mixing can occur, which could mimic a natural wave-wave coupling process in the ambient plasma. Analysis of the effects of the sheath nonlinearities in the instrument response show that when the two sheaths are not identical, one will see a small quadratic nonlinear response proportional to the difference in the floating potentials of the two probes. A typical example of this was seen frequently on both Freja and SCIFER, in the form of a signal at twice the local plasma frequency, and is shown in Figure 1 in an example from Freja. Here in the top panel, we have a 512-μs snapshot of the HF electric field, showing a roughly 10-kHz modulation of a 200 mV/m 250-kHz Langmuir wave, and in the bottom panel, a power spectrum of the electric field showing the primary peak at f_{pe}, and a secondary peak at $2f_{pe}$.

Such a harmonic has been predicted by theory to occur in the coalescence of two Langmuir waves to form an electrostatic or electromagnetic emission at $2f_{pe}$, and has been observed in conjunction with large amplitude Langmuir waves in the solar wind during type III radio bursts [*Cairns and Robinson*, 1992; *Hospodarsky and Gurnett*, 1995]. We were thus quite excited to observe this signal in the data, but our excitement was tempered by the realization that this could be an instrumental effect. The signal at $2f_{pe}$ is down in amplitude by a factor of 30-100 from that at f_{pe}, implying an asymmetry between the floating potentials of the antenna's two probes of this same order of magnitude. Such an

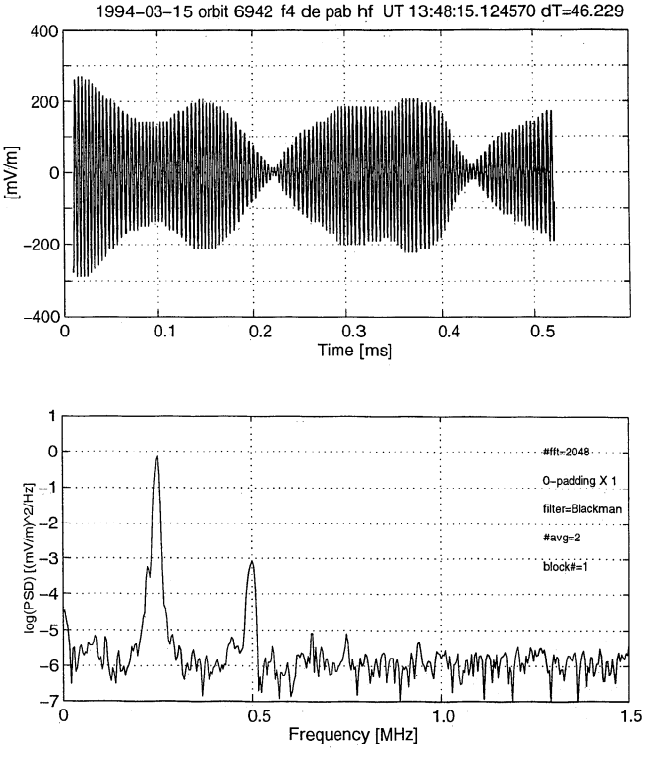

Figure 1. Waveform and power spectrum of HF electric field from Freja, showing modulations of the Langmuir wave envelope, and harmonic signal at $2f_{pe}$.

asymmetry between the probes is plausible, given the possibility of shadowing and surface differences, but is not predictable given the diagnostics available on the antenna. We have confirmed that the signal at $2f_{pe}$ is due primarily to a quadratic interaction by computing the bicoherence [*Kim and Powers*, 1979] for the interaction $f_{pc} + f_{pe} \rightarrow 2f_{pe}$, which is consistent with both a natural wave-wave coupling or an instrumental frequency mixing effect. We cannot further resolve the question of how much of the signal at $2f_{pe}$ could be due to a instrumental effect, but we can use this result as an upper bound on the instrumental nonlinearities.

In the largest amplitude events (≈ 500 mV_{pp}/m), the fluctuating potential across the sheath was on the order of the floating potential. No large signal model for a high frequency sheath exists. Such a sheath structure would certainly produce harmonics, however, and could also produce subharmonics if the change in sheath dimensions with sheath potential were a fractional power. The large signal characteristics of the sheath may also account for the linear scaling of harmonic amplitude with fundamental amplitude seen on both Freja and SCIFER, but this is conjecture.

Low amplitude Langmuir wave events were also studied to look for nonlinearities occurring in the amplifier or digitization electronics. No significant harmonic generation was found, and so we feel that any nonlinearity in the instrument is dominanted by that in the probe sheaths, and that we can estimate an upper bound on its amplitude. Since the harmonic signal is down by a factor of 30-100 from the fundamental, this indicates that a modulation of at most 3 % could be caused by this instrumental non-linearity, which is far smaller than the 50-100 % modulations in amplitude observed in this data set, and which indicates that the observed Langmuir wave modulations are natural in origin.

Description of Modulation Study

Three Freja orbits (89 events; orbits 4862, 5240, 6942) and the entire SCIFER flight (240 events) were manually examined to find cases where the captured waveform was narrow-band and cleanly modulated. It should be pointed out that the presence of amplitude modulated Langmuir waves in these data sets is quite common; i.e. , when we observe Langmuir waves, they invariably have amplitude modulations. Often VLF hiss from 10-kHz upward was present in the signal, in addition to the stronger Langmuir wave emissions. The presence of such low-frequency variations in the baseline of the signal made it difficult to identify periods of modulation, and so a band-pass filter (±100-kHz four-pole digital Butterworth filter around estimated f_{pe}) was applied to the snapshot data to make the modulation envelope clearer, and to prevent these large amplitude, low frequency variations in the baseline from mimicing modulations of the high-frequency signal. The local plasma frequency f_{pe} was then taken as the peak in the spectral density of the electric field. The local electron cyclotron frequency f_{ce} was computed from the on-board dc magnetometers (F2 dc magnetometer on Freja, NASA aspect magnetometer on SCIFER).

The maximum modulation frequency of the Langmuir waves was computed by simply counting the maxima of the wave envelope. Why does this give a good estimate of the modulation bandwidth? Consider a signal at frequency ω_0 modulated at the frequency ω_m,

$$\begin{aligned} x(t) &= \cos\omega_m t \cos\omega_0 t \\ &= (1/2)\{\cos[(\omega_0+\omega_m)t] + \cos[(\omega_0-\omega_m)t]\}. \end{aligned}$$

This signal has two peaks in its frequency spectrum, separated by $2\omega_m$. The maxima of the signal's envelope are separated in time by $\Delta t = \pi/\omega_m = 2\pi/(2\omega_m)$, so counting the maxima in a given snapshot, and dividing by the length of the snapshot gives an estimate of $2\omega_m$, which is the difference in frequency between the two interacting waves. We present an example of this in Figure 2, again taken from Freja. The upper panel is again a 512 μs snapshot of the HF electric field, showing a 32 kHz modulation of a 200 mV/m 510 kHz Langmuir wave, while the lower panel is a power spectrum of the electric field, showing two peaks separated by 32 kHz.

In cases such as this, one can see clear multiple peaks in the power spectrum corresponding to the frequencies of the multiple waves, but in general, the peak is broader and more complicated, which is reflected in the snapshots by a more irregular modulation of the en-

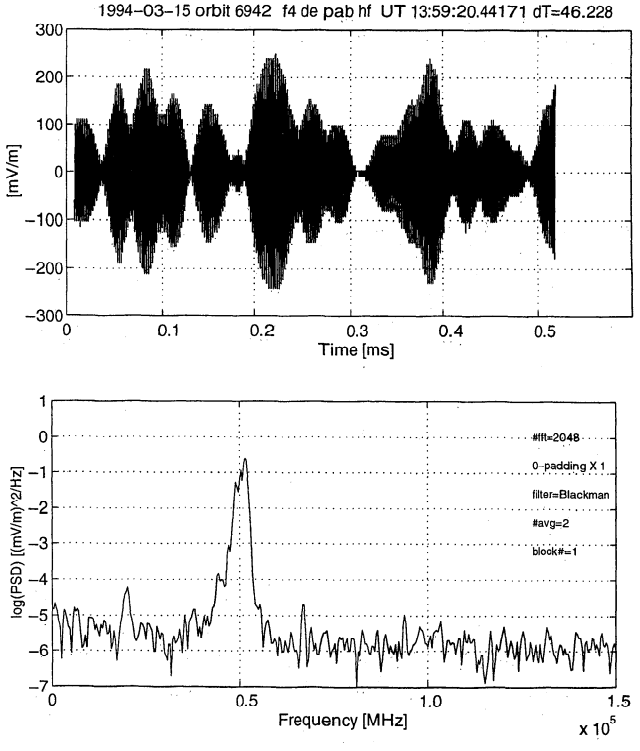

Figure 2. Waveform and power spectrum of modulated Langmuir wave from Freja, showing multiple peaks in power spectrum related to amplitude modulations.

velope. The presence of additional peaks between the maximally-separated peaks contributes to lower modulation frequencies, since the difference in frequency between these peaks is necessarily less than the maximum observed modulation frequency. The computed maximum modulation frequencies were converted to relative modulation frequencies by dividing by f_{pe}.

Because the SCIFER and Freja snapshots were at most 1 ms in length, the minimum observable modulation frequency is $\approx$ 1 kHz. This limit prevents us from reliably observing modulations in the range of frequencies covered by ion acoustic and broadband ELF ($\leq$ several kilohertz), O^+ ($f_{cO+} \approx 30$ Hz) and low order H^+ ($f_{cH+} \approx 430$ Hz) cyclotron and Bernstein modes, but does allow us to observe modulations at the higher frequencies of the electrostatic whistler/lower hybrid mode ($\geq$ several kilohertz). We will find that this lower limit on observable modulation frequency does not preclude the observation of modulations, however, as we have found hundreds of cases where the modulation frequency is several to tens of kilohertz.

Results of Modulation Study

We first show the raw measurements of modulation frequency versus the plasma frequency in Figure 3. Here one can readily see the large number of modulation events at frequencies up to 40 kHz, with a few isolated cases up to 60 kHz. We next show the data as modulation frequency scaled by the plasma frequency versus the parameter $1 - f_{pe}^2/f_{ce}^2$ in Figure 4. We choose this quantity as our independent variable due to the angular dependence of the obliquely propagating Langmuir wave. As was shown by *Newman et al.* [1994a], the dispersion relation for such Langmuir waves has the form,

$$\frac{f}{f_{pe}} \approx 1 + \frac{3}{2}k_{\|}^2\lambda_{De}^2 + \frac{1}{2}\frac{\sin^2\theta}{(f_{pe}^2/f_{ce}^2 - 1)}, \qquad (1)$$

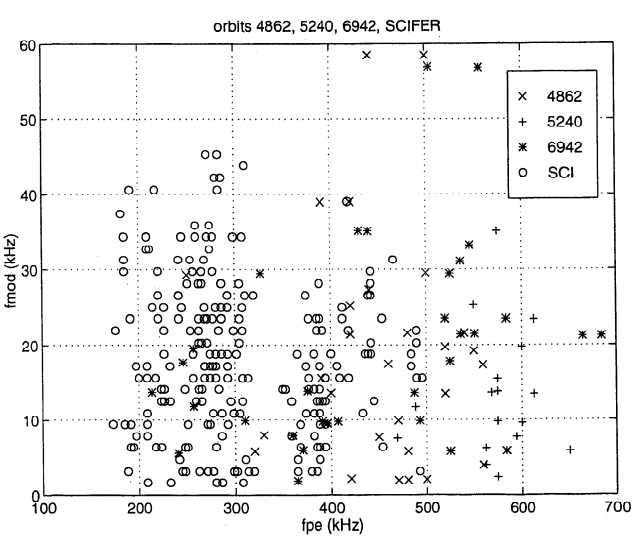

Figure 3. Modulation frequency versus plasma frequency, both in kilohertz for all events in the study.

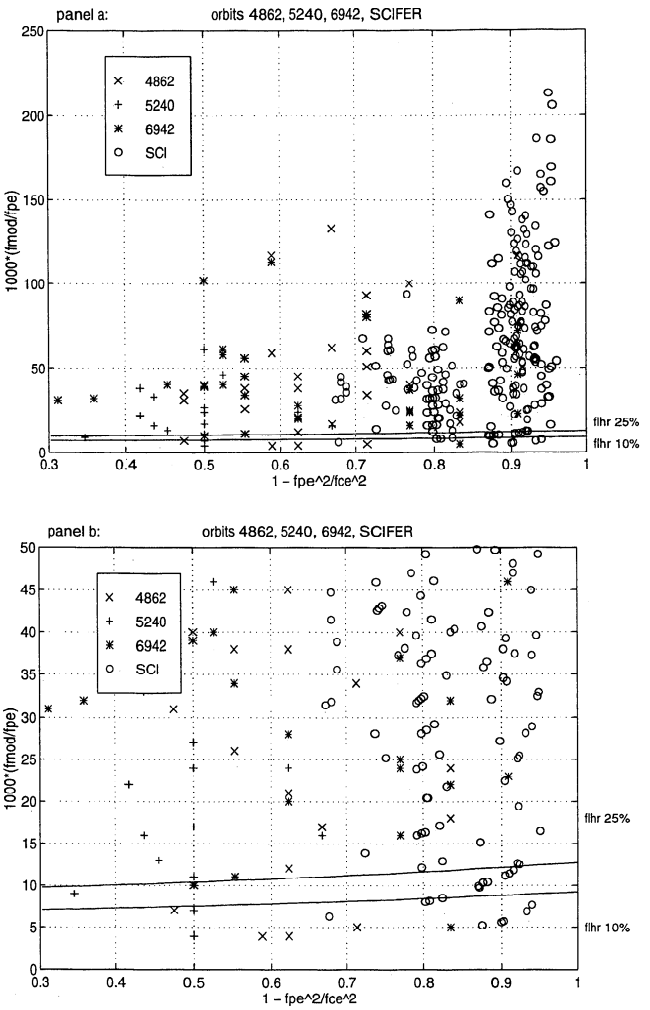

Figure 4. Relative modulation frequency (f_{mod}/f_{pe}) versus oblique Langmuir wave dispersion parameter $1 - f_{pe}^2/f_{ce}^2$. Panel a shows the full range of the modulation frequency, while panel b shows a blowup of the low-frequency regime. Solid curves mark the values of f_{LHR} for 10 % and 25 % H^+ compositions.

for sufficiently small propagation angles and wave numbers ($\tan\theta = k_{\perp}/k_{\|}$; λ_{De} = electron Debye length).

If we are observing modulations of Langmuir waves caused by the beating of two oblique Langmuir waves at different propagation angles, as was suggested by *Newman et al.* [1994b], then the relative modulation frequencies should show some organization based on the oblique Langmuir wave dispersion relation. The primary trend in the data is an increase in the maximum observed relative modulation frequency as the plasma frequency decreases below from the cyclotron frequency (from left to right on Figure 4a). As will be shown below, this is due to an increase in the maximum angle between the two interacting Langmuir waves, rather than a change in the wavenumber between the two waves, due to the far larger effect of propagation angle on the wave frequency than that due to wavenumber. This increase in the spread in angle is most likely due to the decrease in the rate of increase with propagation angle of cy-

clotron damping on scattered electrons at small plasma frequencies, but confirmation of this would require simulation outside the scope of this paper to address fully.

We can compare these data to the modulation frequencies predictable from models involving parametric decay of Langmuir waves with low-frequency ion modes, as well as wave-particle interactions. We will first consider the case of Langmuir wave backscatter off of ion acoustic waves. Then we will consider modulations due to spatial localization of the Langmuir wave packet by kinetic wave-particle interactions. We will then finally consider Langmuir wave modulations due to decay and/or scattering from electrostatic whistler/lower hybrid waves. We will find that the range of modulation frequencies available from the ion acoustic and kinetic wave-particle mechanisms are too small to explain the bulk of the modulation frequencies observed on Freja and SCIFER. However, the range of modulation frequencies available from the electrostatic whistler/lower hybrid mechanism is sufficiently broad as to explain the bulk of the observed modulation frequencies on Freja and SCIFER.

As pointed out by *Newman et al.* [1994b], the frequency shift due to the backscatter decay of a Langmuir wave into another Langmuir wave and an ion acoustic wave is given by $\Delta\omega \approx 2k_1 c_s$. For a beam-driven parent Langmuir wave, $k_1 \approx \omega_{pe}/v_b$, with v_b as the resonant electron speed. Since the ion acoustic speed is $c_s = (T_e/m_i)^{1/2}(1 + T_i/T_e)^{1/2}$, with $1/m_i = (1/n_e)\sum_j n_j/m_j$ for a multi-ion plasma, $\Delta\omega/\omega_{pe} \approx 4(m_e/m_i)^{1/2}(T_e/E_b)^{1/2}$ for $T_e/T_i = 1$. This result gives a maximum frequency shift of $4 \cdot 10^{-3}\omega_{pe}$, for $T_e = 1$ eV, $E_b = m_e v_b^2/2 \geq 100$ eV, and $\epsilon = (m_e/m_i)^{1/2} \approx 10^{-2}$ (10-25 % H^+, remainder O^+). As can be seen in Figure 4b, there are few (20 out of 329) events at such small modulation frequencies. Even if the electron temperature was as high as 10 eV, the ion acoustic backscatter mechanism could only produce modulations of $\leq 10^{-2}\omega_{pe}$, which corresponds to an ordinate of 10 in Figure 4, and which is well below the bulk of the observed modulation frequencies.

Scattering due to parametric decay to ion Bernstein or cyclotron modes will produce modulations at multiples of the particular ion gyrofrequency involved in the decay. At both Freja and SCIFER altitudes, $f_{cO} \approx$ 25-30 Hz, which is far below our minimum observable modulation frequency. The H^+ cyclotron frequency, $f_{cH} \approx$ 430-550 Hz, which would lead to modulation frequencies on the order of $10^{-3} f_{pe}$, corresponding to an ordinate of 1 on Figure 4. Parametric processes involving higher harmonics of f_{cH} may explain some of the lower frequency modulations, but the bulk of the observations would require the excitation of very high ($\geq 10 f_{cH}$) ion harmonics, which would imply high perpendicular wavenumbers and higher thresholds for decay due to increased damping on thermal H^+.

The modulations in Langmuir wave amplitude due to kinetic wave-particle interactions have been shown by *Muschietti et al.* [1995] to be due to spatial modulations of the wave envelope advected across the spacecraft due to the motion of the wave packet. The motion of the wave packet in the spacecraft frame is dominated by its parallel group velocity, which is given by $v_{g||} = \partial\omega/\partial k_{||} \approx 3\omega_{pe} k_{||} \lambda_{De}^2$, using the Bohm-Gross dispersion relation for Langmuir waves. While the perpendicular group velocity of the Langmuir wave packet can be much larger than the parallel due to the angular dependence of the Langmuir wave dispersion relation, all of the structure caused by the wave-particle interaction is in the parallel direction, which precludes advection (and thus amplitude modulation) by $v_{g\perp}$. Again, using the beam-driven condition to estimate the Langmuir wave phase velocity as was done above, and the results of (5) of *Muschietti et al.* [1995], one can show that the relative modulation frequency of the wave packet is,

$$\frac{f_{mod}}{f_{pe}} \approx 3\left(\frac{T_e}{E_b}\right)\left(\frac{\epsilon_0 E_0^2}{2 n_0 E_b}\right)^{1/4}, \qquad (2)$$

with E_0 as the Langmuir wave amplitude and n_0 as the ambient plasma density. For typical values of these parameters ($E_0 = 100$ mV/m, $T_e = 1$ eV, $E_b \geq 100$ eV, $n_0 = 10^3$ cm^{-3}), this kinetic localization process predicts $f_{mod}/f_{pe} \approx 10^{-4}$, which is far smaller than the modulation frequencies observed in this data set.

For modulations caused by parametric processes involving electrostatic whistler/lower hybrid waves (referred to as lower hybrid waves for brevity in what follows), one expects the frequency shifts given by the electrostatic whistler/lower hybrid dispersion relation,

$$\begin{aligned} f_{lh}^2 &= f_{pi}^2(1 + \cos^2\theta)/(1 + f_{pe}^2/f_{ce}^2) \\ &= \epsilon^2 D_{LH}^2(1 + \cos^2\theta/\epsilon^2) f_{pe}^2, \end{aligned} \qquad (3)$$

with $\epsilon^2 = m_e/m_i$, and $D_{LH}^2 = 1/(1 + f_{pe}^2/f_{ce}^2)$, and where the electrostatic ($k_\perp c/\omega_{pe} = k_\perp \lambda_e \gg 1$) and cold ($k_\perp \rho_e \ll 1$) approximation has been used ($\lambda_e =$ electron skin depth; $\rho_e =$ electron gyroradius). The minimum frequency shift possible from the lower hybrid mode is the lower hybrid resonance frequency, $f_{LHR} = \epsilon D_{LH} f_{pe}$, and is plotted in both panels of Figure 4 for both 10 % and 25 % H^+ ion compositions. As can be seen, only 20 of the 329 total events from this study lie below f_{LHR} and thus represent events which can not be explained via a Langmuir-lower hybrid wave interaction. This observation frequency should not be taken as a true estimate of the occurrence rate on non-lower hybrid processes due to the observational biases caused by snapshot length discussed above. The full range of modulation frequencies observed in this data set can be explained by parametric processes occurring at frequencies of (1-20)f_{LHR}, with the larger frequencies required at smaller plasma frequencies as noted above. This range of frequencies corresponds to lower hybrid waves at angles less than 11.5 deg (0.2 rad) away from perpendicular.

In summary, we see that while three-wave processes involving Langmuir wave interactions with ion acous-

tic and ion cyclotron waves may explain the lowest observed modulation frequencies, they can not explain the bulk of the observed higher frequency modulations of the Langmuir waves. One also sees this same result when considering kinetic wave-particle mechanisms of Langmuir wave modulation; ie. the resulting modulation frequencies are too low to explain the bulk of the observed Langmuir wave modulations. Finally, one sees that a mechanism involving three-wave interactions between Langmuir waves and electrostatic whistler/lower hybrid waves can readily explain the entire range of observed modulation frequencies, except for the very lowest. We will now consider the further ramifications of such a model for the modulated Langmuir waves.

Langmuir-Lower Hybrid Wave Interaction Model

Observations indicating that electrostatic whistler /lower hybrid waves were involved in Langmuir wave modulations have been published before [*Ergun et al.*, 1991; *Kellogg et al.*, 1992; *Sharma et al.*, 1992; *Stasiewitz et al.*, 1996] and our $\approx$ 300 observations serve to confirm that possibility. While the Langmuir/lower hybrid coupling can clearly explain the observed modulation frequencies of the Langmuir waves, we have to consider whether such an interaction is plausible kinematically and physically, given the dispersion relations governing the two modes involved, and our observations of the electric fields of the modulated Langmuir waves and at the frequency of modulation.

It is an unavoidable experimental fact that we do not see a clear coincidence between electric field power in modulated Langmuir waves, and power at the frequency of modulation itself. The question of the relationship between power at Langmuir wave frequencies and at lower frequencies will be dealt with in greater detail over a larger data set in a subsequent paper (J.-E. Wahlund et al., manuscript in preparation, 1997), but for the particular cases shown in this study, we can say that there is little or no power (typically $\leq$ 5 mV/m amplitudes) at low frequencies in the Freja observations, as can be seen in Figure 2, which shows a typical spectrum with little or no power below 100 kHz, even considering the roll off of this channel's response below 100 kHz. The SCIFER observations show similar amounts of broadband power over a frequency band covering the range of modulation frequencies of the Langmuir waves, but no detailed correlation in time between enhancements in modulated Langmuir wave power, and narrow-band enhancements in VLF hiss power.

These observations suggest that either the power at the modulation frequency produced by the decay of the Langmuir wave is quite small, or the amplitude of the electric field at the modulation frequency required to scatter the Langmuir wave is also quite small. Depending upon the details of the final state of the scattering process, these possibilities are consistent with the observed lack of correlation.

Another point to consider is that once the Langmuir wave has scattered some of it power into an oblique Langmuir wave and lower hybrid wave, the group velocities of the resulting waves would lie in quite different directions, with the group velocity of the lower hybrid waves directed predominantly along the magnetic field, and that of the Langmuir waves directed across the magnetic field. A possible scenario is thus that the initial Langmuir wave is generated in a particular spatial region, partially scatters and/or decays to produce an oblique Langmuir wave and lower hybrid wave. The two Langmuir waves then exit the generation region off to the side, while the lower hybrid wave proceeds down the field line. The observed modulated Langmuir waves would then be the two uncoupled obliquely propagating Langmuir waves beating against each other. In this scenario, we rarely observe the actual interaction region, but instead observe the products of the interaction, namely two Langmuir waves with similar amplitudes and closely spaced frequencies.

We would like to determine the wave numbers of the resultant lower hybrid and oblique Langmuir waves due to the parametric decay of a parent beam-driven Langmuir wave. From this we will show that the resonant lower hybrid waves fit the cold electrostatic dispersion relation, and have phase velocities which preclude strong damping on ambient particle populations.

Using the lower hybrid,

$$f_{LH}/f_{pe} = \epsilon D_{LH}(1+a^2)^{1/2}, \tag{4}$$

and oblique Langmuir wave,

$$f_L/f_{pe} \approx 1 + \frac{3}{2}k_{||}^2\lambda_{De}^2 + \frac{D_L^2}{2}\sin^2\theta_L, \tag{5}$$

dispersion relations, where

$$\begin{aligned} a &= \cos\theta_{LH}/\epsilon, \\ D_L^2 &= 1/(f_{pe}^2/f_{ce}^2 - 1), \end{aligned}$$

and where we have assumed that $k_{||}^2\lambda_{De}^2 \ll 1$ and $|D_L^2 \sin^2\theta_L/2| \ll 1$, we can then plug into the usual resonant three-wave frequency and wavevector matching conditions, and solve for the properties of the daughter Langmuir and lower hybrid waves in terms of the observed modulation frequency and parent Langmuir wavevector. Figure 5 shows the wavevector geometry for the parametric decay of the initially parallel propagating, beam-driven Langmuir wave to an oblique Langmuir wave and lower hybrid wave in both the $k_{||} > 0$ and $k_{||} < 0$ cases of the lower hybrid wave. Note that this is a direct scatter to finite $k_\perp$, rather than a random walk to finite $k_\perp$ through multiple, small-angle ion acoustic backscattering events, as would be required by a Langmuir- ion acoustic interaction.

Our resonance conditions from $\omega_1 = \omega_2 + \omega_{LH}$ and $\mathbf{k}_1 = \mathbf{k}_2 + \mathbf{k}_{LH}$ are as follows:

$$1+\frac{3}{2}k_1^2\lambda_{De}^2 = 1+\frac{3}{2}k_2^2\lambda_{De}^2+\frac{D_L^2}{2}\sin^2\theta_2 + \epsilon D_{LH}(1+a^2)^{1/2}, \quad (6a)$$

$$k_1 = k_2\cos\theta_2 + k_{LH}\cos\theta_{LH}, \quad (6b)$$

$$0 = k_2\sin\theta_2 + k_{LH}\sin\theta_{LH}, \quad (6c)$$

where we have assumed that $\sin^2\theta_2 \ll 1$ so that $\cos^2\theta_2 \approx 1$. These resonance relations can be combined to get a fourth-order polynomial in k_{LH} as a function of k_1, the frequency shift, and the ambient plasma parameters (through D_{LH} and D_L^2). This fourth-order equation can be reduced to a biquadratic form (second-order in k_{LH}^2) by assuming that the daughter Langmuir and lower hybrid wavevectors are orthogonal to each other. This restricts us to considering the forward propagating lower hybrid case, which should be preferred due to its smaller wavenumber, higher phase velocity, and resultant reduced damping, as can be seen by inspection of Figure 5. Keeping the entire fourth-order equation only produces a correction of ≈ 10 % to the results, and the simplified form is easier to work with, so we will proceed with it in the following analysis.

The wavenumber of the resonant lower hybrid wave is given by $k_{LH}^2 = k_1^2 \cdot 2\epsilon(1+a^2)^{1/2}D_{LH}/|D_L^2|$, and that of the resonant oblique Langmuir wave $k_2^2 \approx k_1^2$. For resonant electron energies of 100-1000 eV, these resonance conditions predict $k_{LH}^2c^2/\omega_{pe}^2 \geq 20$, and $k_{LH}^2\rho_e^2 \leq 4\cdot 10^{-3}$ which are comfortably within the cold, electrostatic model assumed for the lower hybrid waves. The perpendicular phase velocity of the lower hybrid waves is $\omega_{LH}^2/k_{LH}^2 \approx v_b^2\epsilon D_{LH}|D_L^2|(1+a^2)^{1/2}$, which would predict resonance with electrons at energies of 0.1-0.01 times the driving beam energies, with the smaller resonance energies associated with smaller modulation frequencies. For driving electron energies of a few hundred eV, the resultant lower hybrid waves will be resonant with electrons well out on the thermal tail, and should not experience excessive damping.

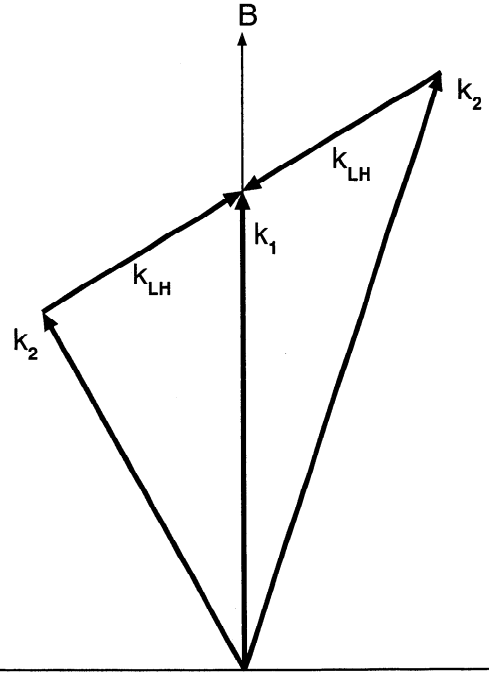

Figure 5. Wavevector geometry for parametric decay of a Langmuir wave to an oblique Langmuir wave and lower hybrid wave. The parent Langmuir wave has frequency and wave vector $(\omega_1, \mathbf{k}_1)$, the daughter Langmuir wave $(\omega_2, \mathbf{k}_2)$, and the daughter lower hybrid wave $(\omega_{LH}, \mathbf{k}_{LH})$.

There are no obvious properties of the daughter waves which would explain the increased modulation frequencies observed at small plasma frequencies, and so this effect must be due to the dynamics of the actual decay process, possibly involving the damping rates of the oblique Langmuir waves as discussed above. In addition, as the plasma frequency drops, the dispersion relation of the oblique Langmuir waves approaches the form $\omega_L = \omega_{pe}\cos\theta_L = \omega_{pe}k_{||}/k$. This can be rearranged to the form $\omega/k_{||} = \omega_{pe}/k$ so that if the k of the daughter Langmuir wave stays the same as that of the parent, beam-driven Langmuir wave, the daughter wave will remain in resonance with the electron beam, and the decay to that mode will be enhanced. Since the resonance conditions predict that the wavenumber of the oblique Langmuir wave remains the same as the parent, this property of the interaction can contribute to the enhanced modulation bandwidth at small plasma frequencies.

One can also see that the side-scattering is at least possible dynamically by examining the structure of the electron continuity and momentum equations. If one were to only have vector nonlinearities, such as the convective nonlinearity in the momentum equation, then purely perpendicular side-scatter of the Langmuir wave would not be possible in the weak-turbulence limit because the perturbed velocities of the Langmuir and lower hybrid waves would be orthogonal. However, there exist scalar nonlinearities in the continuity equation driven by the divergence term, which do not depend upon the angle between the Langmuir and lower hybrid waves, and which allow for direct side-scatter.

Our observations of scattering at large angles do not preclude scattering at smaller angles. In regimes where $f_{pe} \approx f_{ce}$, the scattering region will have a reduced range in angle, as was shown by *Newman et al.* [1994b], and will prefer the ion acoustic backscatter process. One can also presume that the small-angle scattering proceeds in parallel to any large-angle scattering, but that the limitations of the Freja and SCIFER datasets discussed above preclude our observations of it. Nevertheless, our observations show that there is a large population of modulated Langmuir wave events which can not be explained via the ion acoustic backscatter process, and thus require the larger frequency shifts possible via the Langmuir/lower hybrid interaction.

Conclusions

We have shown from a substantial data set of modulated Langmuir wave events gathered from both satel-

lite and sounding rocket instruments in the auroral zone that the scattering or decay of Langmuir waves via electrostatic whistler/lower hybrid waves is an important component of Langmuir wave dynamics in that region. Application of the basic three-wave resonance conditions to such a parametric decay show that lower hybrid waves in the cold electrostatic limit can produce the observed modulation frequencies. The necessary amplitudes for both the Langmuir and lower hybrid waves to participate in this decay and scattering process are not derivable from the resonance conditions and will require further analysis and simulation to uncover.

Acknowledgments. The work of J. Bonnell, P. Kintner, and J.-E. Wahlund was supported by ONR grant N00014-92-J-1822 and NASA grant NAG 5-691. The work of J. A. Holtet was supported by a grant from The Research Council of Norway. The Freja project was supported by the Swedish National Space Board (SNSB) and by the Deutsche Agentur für Raumfahrtangelegenheiten (DARA). J.B. would like to acknowledge illuminating discussions on three-wave processes with M. Goldman, and wave-particle interactions with L. Muschietti.

The Editor thanks D. Gallagher and another referee for their assistance in evaluating this paper.

References

Akimoto, K., Y. Omura, and H. Matsumoto, Rapid generation of Langmuir wave packets during electron beam-plasma instabilities, *Phys. Plasmas*, *3*, 2559, 1996.

Boehm, M. H., C. W. Carlson, J. P. McFadden, J. H. Clemmons, R. E. Ergun, and F. S. Mozer, Wave rectification in plasma sheaths surrounding electric field antennas, *J. Geophys. Res.*, *99*(A11), 21361–21374, 1994.

Cairns, I. H., and P. A. Robinson, Theory for low-frequency modulated Langmuir wave packets, *Geophys. Res. Lett.*, *19*, 2187, 1992.

Ergun, R. E., C. W. Carlson, J. P. McFadden, J. H. Clemmons, and M. H. Boehm, Evidence of a transverse modulational instability in a space plasma, *Geophys. Res. Lett.*, *18*, 1177, 1991.

Hospodarsky, G. B., and D. A. Gurnett, Beat-type Langmuir wave emissions associated with a type III solar radio burst: Evidence of parametric decay, *Geophys. Res. Lett.*, *22*, 1161–1164, 1995.

Kellogg, P. J., K. Goetz, N. Lin, S. J. Monson, A. Balogh, R. J. Forsyth, and R. G. Stone, Low frequency magnetic signals associated with Langmuir waves, *Geophys. Res. Lett.*, *19*, 1299, 1992.

Kim, Y., and E. Powers, Digital bispectral analysis and its application to nonlinear wave interactions, *IEEE Trans. Plasma Sci.*, *1*, 120, 1979.

Kintner, P. M., J. Bonnell, S. Powell, J.-E. Wahlund, and B. Holback, First results from the Freja HF snapshot receiver, *Geophys. Res. Lett.*, *22*, 287, 1995.

Maggs, J. E., Electrostatic noise generated by the auroral electron beam, *J. Geophys. Res.*, *83*, 3173, 1978.

McFadden, J. P., C. W. Carlson, and M. H. Boehm, High-frequency waves generated by auroral electrons, *J. Geophys. Res.*, *91*, 12079, 1986.

Muschietti, L., I. Roth, and R. E. Ergun, Kinetic localization of beam-driven Langmuir waves, *J. Geophys. Res.*, *100*, 17481, 1995.

Newman, D. L., M. V. Goldman, R. E. Ergun, and M. H. Boehm, Langmuir turbulence in the auroral ionosphere, 1, Linear theory, *J. Geophys. Res.*, *99*, 6367, 1994a.

Newman, D. L., M. V. Goldman, R. E. Ergun, and M. H. Boehm, Langmuir turbulence in the auroral ionosphere, 2, Nonlinear theory and simulations, *J. Geophys. Res.*, *99*, 6377, 1994b.

Sharma, R. P., Y. K. Tripathi, A. H. A. Janabi, and R. W. Boswell, Parametric excitation of electrostatic whistler waves by electron plasma waves, *J. Geophys. Res.*, *97*, 4275, 1992.

Stasiewitz, K., B. Holback, V. Krasnoselskikh, M. Boehm, R. Böstrom, and P. M. Kintner, Parametric instabilities of Langmuir waves observed by Freja, *J. Geophys. Res.*, *101*, 21515, 1996.

J. Bonnell and P. Kintner, 303 Rhodes Hall, Cornell University, Ithaca, NY 14850 (johnb@ee.cornell.edu; paul@ee.cornell.edu)

J.-E. Wahlund, Swedish Institute of Space Physics, Kiruna Division, S-755 91 Uppsala SWEDEN (jwe@irfu.se)

J. A. Holtet, Dept. of Physics, University of Oslo, PO. Box 1048 Blindern, N-0316 Oslo, Norway (j.a.holtet@fys.uio.no)

(Received March 10, 1997; revised May 16, 1997; accepted May 19, 1997.)